

# Reduction of stress and roughness by reactive sputtering in W/B<sub>4</sub>C X-ray multilayer films

David L. Windt

Reflective X-ray Optics LLC, 1361 Amsterdam Ave., Suite 3B, New York, NY 10027

## ABSTRACT

We have investigated the stress and roughness in W/B<sub>4</sub>C X-ray multilayer films grown by reactive DC magnetron sputtering in a nitrogen-argon gas mixture. We have also studied the properties of single-layer W and B<sub>4</sub>C films, in order to understand specifically how the stress, roughness, chemical composition and microstructure in these materials depends on the sputter gas composition. We find that the stress and roughness in both single-layer and multilayer films deposited reactively is reduced substantially; we find a corresponding improvement in X-ray performance in the case of multilayer films designed to operate at X-ray energies for which the incorporation of nitrogen will not adversely affect the optical properties of these coatings. Furthermore, the observed reduction in film stress in these coatings will mitigate stress-driven adhesion failures. In the case of single-layer W films, the observed reduction in stress and roughness is correlated with a change in microstructure: the W film is amorphous when deposited reactively (and contains ~12–25% incorporated N, depending on the sputter gas composition), versus polycrystalline when deposited in pure argon gas. Finally, we find extremely low surface roughness in reactively-sputtered films of amorphous B<sub>4</sub>CN<sub>x</sub>; thus, in addition to their use in X-ray multilayer reflective coatings, these films can be used as smoothing layers to reduce the surface roughness of X-ray mirror substrates, thereby leading to reduced scattering and higher specular reflectance.

**Keywords:** Multilayers, X-rays, Reactive Sputtering

## 1. INTRODUCTION

Nanometer-scale multilayer thin films are by now widely used in a variety of scientific and industrial applications as reflective mirror coatings operating in the EUV, soft X-ray and hard X-ray bands. The performance of these coatings depends crucially on the smoothness of the interfaces between each layer comprising the stack, as interfacial roughness will scatter X-rays into non-specular directions thereby reducing the net specular reflectance. The surface roughness of the underlying substrate is also crucially important, since the substrate roughness can be replicated at each interface in the multilayer stack, also leading to increased scattering and reduced reflectance.<sup>1,2</sup> Film stress is an additional critical parameter that must be minimized in order to avoid coating adhesion failure, substrate distortion and other problems.<sup>3</sup>

Many deposition and film growth techniques have been investigated with the aim of reducing roughness and film stress in X-ray multilayers. However a single deposition technique that reduces roughness and stress simultaneously has proven somewhat elusive, as these two characteristics are often inversely correlated with each other, particularly in the case of commonly used X-ray multilayer structures such as Mo/Si, W/Si, W/B<sub>4</sub>C, etc. typically grown by magnetron sputtering. The inverse correlation between film stress and surface roughness occurring commonly in sputtered films can be understood as a manifestation of the microstructure of the individual layers: in the context of the structure-zone model described by Thornton<sup>4</sup> (and revised by Messier et al<sup>5</sup>), the smoothest sputtered films are characterized by a zone T-type microstructure comprising tightly packed columnar grains, an over-dense structure with large compressive stresses; as the deposition conditions change (for example, by increasing the sputter gas pressure) so as to produce films having lower (compressive) stresses, the film tends towards the zone 1-type microstructure characterized by porous columnar grains with large surface roughness, ultimately producing tensile stresses due to attractive forces between the columnar grains.

We describe here an investigation of stress and roughness in X-ray multilayer structures grown by reactive DC magnetron sputtering using a nitrogen-argon gas mixture. The overall aim of this effort is to determine if reactive sputtering with nitrogen can be used to simultaneously reduce stress and roughness in these films, thereby leading to better performance. In particular, we have studied both periodic and depth-graded W/B<sub>4</sub>C multilayers. We have also studied the properties of single-layer W and B<sub>4</sub>C films, in order to understand specifically how the stress, roughness,

chemical composition and microstructure in these materials depends on the sputter gas composition. We recognize that reactive sputtering with nitrogen will result in the incorporation of nitrogen in the films, which will degrade multilayer optical performance in the EUV where nitrogen is strongly absorbing. But the incorporation of nitrogen will have little, if any, effect on the optical constants of these materials at shorter wavelengths in the soft and hard X-ray bands; we are thus focusing on multilayers that would be suitable for use at shorter X-ray wavelengths where nitrogen incorporation is not problematic.

The W/B<sub>4</sub>C multilayer system selected for study here is potentially important for both normal-incidence applications in the soft X-ray band using periodic structures, and for grazing-incidence applications in the hard X-ray for which depth-graded structures are required to achieve broad-energy response. Ultra-short period, narrow-band W/B<sub>4</sub>C multilayers have already been shown to work reasonably well at wavelengths in the 1.5 – 2.5 nm range near normal incidence,<sup>6</sup> yet the performance of these films could be improved further if the interfacial roughness in these structures could be reduced. We have also previously produced prototype depth-graded W/B<sub>4</sub>C multilayers, however the large stresses in these coatings have precluded their use thus far, as films deposited onto figured thin glass substrates (as would be used in the construction of astronomical multilayer X-ray telescopes, for example,) have suffered catastrophic stress-driven adhesion failures.<sup>7</sup>

In the following sections we describe the details of our investigation, specifically (a) the experimental techniques used for film growth and characterization, (b) the experimental results demonstrating the effects of reactive sputtering, and (c) a discussion of these results and how they may be exploited for improved performance of multilayer X-ray optics. We conclude with a summary of our findings and a brief outline of prospects for future investigations.

## 2. EXPERIMENTAL

### 2.1 Film Deposition

All films studied here were deposited by DC magnetron sputtering in one of two separate deposition systems. The first system<sup>8</sup> – the so-called “Vactec” system – utilizes 50.8 cm x 8.9 cm rectangular planar magnetron cathodes. The cathodes are arranged along the diagonal of the square vacuum chamber and sputter up, while the substrate faces down as it rotates past each cathode. The computer-controlled substrate rotational velocity is used to control individual layer thicknesses (i.e., faster rotation produces thinner layers.) The substrate also spins at ~230 rpm as it rotates, in order to improve coating thickness uniformity. The cathodes are powered by regulated DC power supplies (Advanced Energy model MDX 5K) operated in constant-power mode. The vacuum chamber is cryo-pumped and can reach an ultimate base pressure of less than 3.0x10<sup>-8</sup> Torr; the films discussed below were deposited after pumping for ~24 hours, at which time the chamber background pressure was typically in the range 1 – 2 x10<sup>-7</sup> Torr. The working gas is introduced into the vacuum chamber during sputtering using mass flow controllers (MKS model 2259C) that are operated in a closed-loop feedback configuration set to operate at a constant total gas pressure as measured by a high-precision capacitance manometer (MKS model 390HA). All films deposited in the Vactec system were grown using a total sputter gas pressure of 1.6 mTorr, with a target-to-substrate distance of 10 cm. For non-reactive sputtering, argon of 99.998% purity was used with a resultant flow rate of ~280 sccm. For reactive sputtering with nitrogen, N<sub>2</sub> gas of 99.998% purity was used and the N<sub>2</sub> flow rate was set manually; the Ar flow rate was automatically reduced accordingly in order to maintain a constant total gas pressure. Table 1 lists the Ar and N<sub>2</sub> flow rates, along with the effective “N<sub>2</sub> Gas Fraction”, which we define as the N<sub>2</sub> flow rate divided by the total Ar + N<sub>2</sub> flow rates. Also listed are Ar and N gas concentrations in the vacuum chamber as determined using a residual gas analyzer (Stanford Research Systems model RGA 200.) All films grown in the Vactec system were made with the W cathode operating at 100W and the B<sub>4</sub>C cathode at 500W.

**Table 1.** Ar and N<sub>2</sub> flow rates used for samples prepared in the Vactec deposition system. The ‘N<sub>2</sub> Gas Fraction’ is defined as the N<sub>2</sub> flow rate divided by the sum of the Ar + N<sub>2</sub> flow rates. The Ar and N concentrations were determined from RGA measurements.

Ar Flow Rate [sccm]	N <sub>2</sub> Flow Rate [sccm]	N <sub>2</sub> Gas Fraction	Ar Concentration	N Concentration
283	0	0%	95.0%	0.5%
263	25	9%	89.8%	4.7%
241	50	17%	82.9%	10.1%
223	75	25%	76.0%	15.0%
199	100	33%	69.5%	21.0%

The second deposition system used to produce some of the films studied here utilizes 4.5 cm diameter circular “S-Gun” magnetron cathodes, which comprise a concentric anode-cathode configuration.<sup>9</sup> The S-Gun system is similar to the Vactec system just described, in that the cathodes sputter up and the substrate spins as it rotates over the cathodes; the cathodes are again operated in constant-power mode using precision power supplies (Advanced Energy model MDX 500), and gas flow is controlled at constant total gas pressure using a closed-loop feedback configuration employing mass flow controllers and a capacitance manometer (the same model MKS items noted above.) The S-gun system is pumped using both a turbo- and a cryo-pump, and all samples were deposited after ~24 hours pumpdown, thereby reaching a background pressure in the range  $2\text{--}3 \times 10^{-7}$  Torr. The S-gun films were deposited at a total gas pressure of 2.0 mTorr, with an 8-cm target-to-substrate distance. (Thus the pressure-distance product is the same in both systems: the pressure-distance product is, in fact, the parameter that largely drives the momentum transferred to adatoms on the surface of the growing film from energetic ions and gas atoms; momentum transfer has a large effect on the resultant microstructure.<sup>10</sup>) Table 2 lists the Ar and N<sub>2</sub> flow rates, and the N<sub>2</sub> Gas Fraction (as defined above) as well, for the S-Gun system. Unfortunately the S-gun system is not fitted with an RGA, so no gas concentration measurements were available. For the work described here, the W cathode was operated at 40W power, while the B<sub>4</sub>C cathode at 60W.

**Table 2.** Ar and N<sub>2</sub> flow rates used for samples prepared in the S-Gun deposition system.

Ar Flow Rate [sccm]	N <sub>2</sub> Flow Rate [sccm]	N <sub>2</sub> Gas Fraction
33.70	0	0%
31.99	2.20	6.4%
30.28	4.15	12.1%
28.57	5.86	17.0%
27.35	7.33	21.4%
26.13	8.79	25.2%
24.91	10.01	28.7%

## 2.2 X-ray Analysis

Grazing incidence X-ray reflectance (XRR) measurements were made in the  $\theta$ - $2\theta$  geometry using an X-ray diffractometer comprising a sealed-tube Cu anode operating at 1.3 kW, and a Ge crystal monochromator tuned to the Cu K- $\alpha$  line (8 keV). The sample and detector are positioned using a 4-circle Huber goniometer. Fits<sup>11</sup> to the measured XRR data were used to determine film thicknesses in the case of single-layer films, and the multilayer period  $d$  in the case of periodic multilayer films. X-ray diffraction (XRD) measurements were made using the same system for selected samples as described below, also in the  $\theta$ - $2\theta$  geometry.

## 2.3 Atomic Force Microscopy

The surface roughness of selected samples was measured using an atomic force microscope (Veeco model Nanoscope IIIa controller, with Dimension 3100 microscope and Dimension AFM Scan Head). The AFM measurements were made in ‘tapping-mode’ using a Si probe tip (Veeco model TESP7), with 512 points acquired over a 2  $\mu\text{m}$  scan length, corresponding to spatial frequencies in the range  $0.5\text{--}128\ \mu\text{m}^{-1}$ . The radially-averaged Power-Spectral-Density (PSD) function was computed from the 2D AFM data using the TOPO software package.<sup>12</sup>

## 2.4 Film Stress

Film stress was measured using a wafer curvature system (Toho Technologies model Flexus 2320S.) Selected samples were deposited onto 75-mm Si (100) wafers of nominal 0.4 mm thickness, and the wafer curvature was measured before and after film deposition. The total film thickness as determined by XRR was used to compute film stress, following the standard formalism based on the Stoney equation.<sup>13</sup> In addition, stress-vs-temperature measurements, from room-temperature (25C) to 300C, were made on selected multilayer samples using the same instrument.

## 2.5 X-ray Photoelectron Spectroscopy

X-ray Photoelectron Spectroscopy (XPS) measurements were made on selected W and B<sub>4</sub>C films in order to determine the concentrations of incorporated nitrogen as a function of N<sub>2</sub> Gas Fraction. The XPS measurements were made by

Evans Analytical Group (Hightstown, NJ), with a Phi 5701 LSci system using Al K $\alpha$  X-rays (1.4866 keV). Depth-profiling was achieved via Ar ion sputtering.

### 3. RESULTS

#### 3.1 Single-Layer Films of W and B<sub>4</sub>C

Single-layer films of W and B<sub>4</sub>C were first deposited in the S-Gun system described above onto 75-mm diameter Si (100) wafers, at each of the N<sub>2</sub> Gas Fraction values listed in Table 2. A total of (7) W and (7) B<sub>4</sub>C films were thus deposited. Apart from the systematic variation in N<sub>2</sub> flow rate, from 0 to 10 sccm, all other deposition conditions were held constant, as per the general description provided in the previous section. Film thicknesses were determined using XRR; the film thicknesses thus determined for the W and B<sub>4</sub>C films deposited using pure Ar gas were 24.1 nm and 32.4 nm, respectively, and the thicknesses measured for the remaining films (i.e., deposited reactively) monotonically decreased, in the case of W, and monotonically increased, in the case of B<sub>4</sub>C. Film thicknesses were used to compute the relative deposition rate variations with N<sub>2</sub> Gas Fraction, which are shown in Figure 1a. A large increase in B<sub>4</sub>C deposition rate with N<sub>2</sub> Gas Fraction was observed, which is in fact highly advantageous given the very low intrinsic sputtering rate for pure B<sub>4</sub>C that is generally a rate-limiting factor in the fabrication of B<sub>4</sub>C-based multilayers. While the W deposition rate decreases with N<sub>2</sub> Gas Fraction, the lower W rates are not problematic given the relatively high intrinsic W sputter rate, and the greater heat capacity of the W target which affords relatively high cathode powers if necessary.

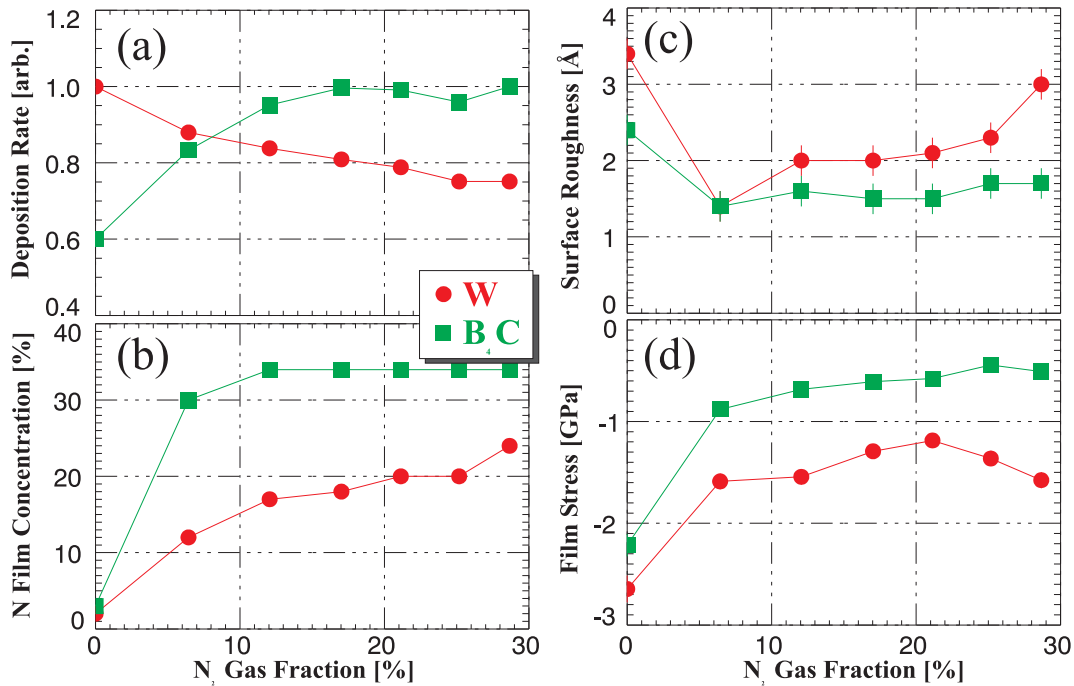


**Figure 1.** (a) Concentration of nitrogen from XPS measurements (b) deposition rate, (c) surface roughness, and (d) film stress as a function of N<sub>2</sub> Gas Fraction for W (circles) and B<sub>4</sub>C (squares) films.

Also shown in Fig. 1 are the average nitrogen concentrations determined by XPS (Fig. 1b), the rms surface roughnesses determined from AFM measurements (Fig. 1c), and the film stresses determined by wafer curvature (Fig. 1d). From the XPS data it is clear that the N concentration increases steadily with N<sub>2</sub> Gas Fraction in the case of the W films, reaching a maximum value of ~25%; the W films are thus non-stoichiometric nitrides, in general, which we designate henceforth as WN<sub>x</sub>. In contrast, the N concentration saturates at 34% once the N<sub>2</sub> Gas Fraction has reached a value of 12% in the case of the B<sub>4</sub>C films. XPS results also indicate that the B:C concentration ratio is ~4:1 for all films, so that the films comprise near-stoichiometric B<sub>4</sub>C regardless of the amount of N also included. For simplicity, we henceforth designate these films as B<sub>4</sub>CN<sub>x</sub>.

As can be seen from the rms surface roughness values shown in Fig. 1c, there is a sharp and significant reduction in surface roughness in both the  $WN_x$  and  $B_4CN_x$  films relative to the pure W and  $B_4C$  films. There is also a corresponding large decrease in compressive stresses. In particular, the  $B_4C$  film has a stress of  $-2.2$  GPa, but the  $B_4CN_x$  films all have stresses below  $-1$  GPa; similarly the W film has a stress of  $-2.6$  GPa while the  $WN_x$  films have stresses below  $-1.5$  GPa.

The AFM data also reveals a marked change in the surface topography of the W vs.  $WN_x$  films. Shown in Figure 2a are AFM scans for a 100-nm-thick W film and a 100-nm-thick  $WN_x$  film deposited in the Vactec system with an  $N_2$  Gas Fraction of 9%; the corresponding PSD curves are shown in Fig. 2b. The W film has a relatively large rms surface roughness ( $\sigma=8.63\text{\AA}$ ), and the surface topography reveals a large number of deep ‘holes’, roughly  $0.1\ \mu\text{m}$  in diameter. In contrast, the  $WN_x$  film is much smoother ( $\sigma=2.62\text{\AA}$ ), and shows nearly homogeneous topography. (The white ‘spots’ in these AFM images are due to dust on the sample surface.) From Fig. 2b we see also that the reduction in surface roughness occurs over the entire range of spatial frequencies sampled. (Note that we find a steady increase in rms surface roughness with film thickness in these W films, which explains why the rms roughness values are so much higher than the values measured for the much thinner films presented in Fig. 1.)

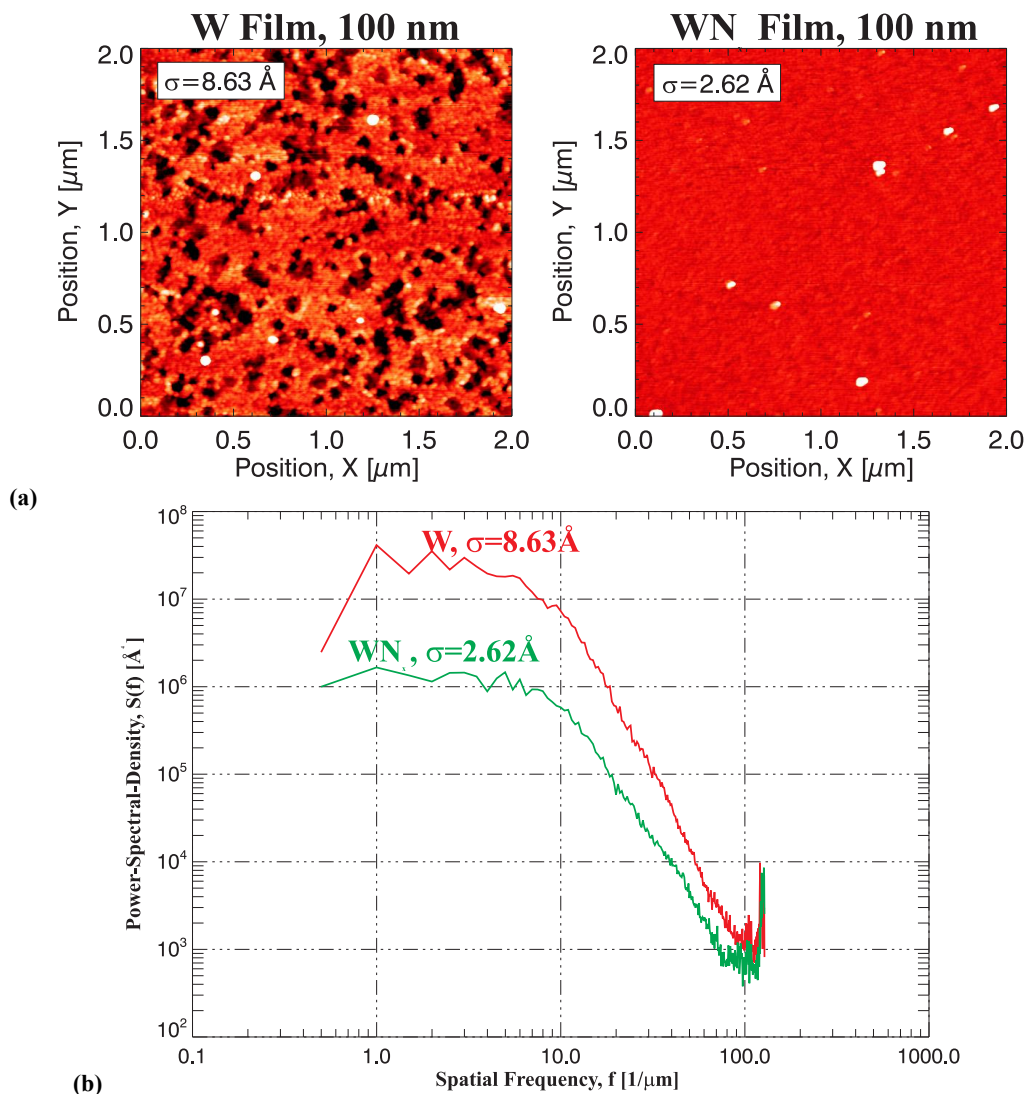


**Figure 2.** (a) Atomic force microscope images and (b) Power-Spectral-Density curves for 100-nm-thick W and  $WN_x$  films, as labeled.

XRD measurements were made for the films shown in Figure 2, and the results are shown in Figure 3 where we plot X-ray intensity vs.  $2\theta$  from  $35^\circ$  to  $60^\circ$ . The strong peak near  $2\theta=40.5^\circ$  in the W film is due to diffraction from the bcc W (110) lattice planes; this peak is completely absent in the data for the  $WN_x$  film, suggesting an amorphous microstructure. The variation in surface topography in these films (Fig. 2) is presumably correlated with the polycrystalline vs. amorphous microstructure suggested by the XRD data.

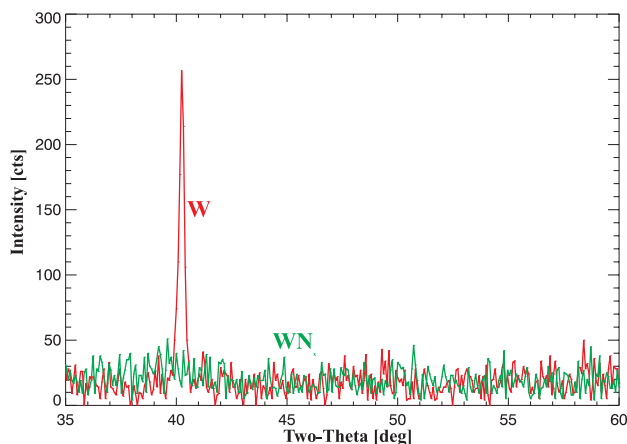


**Figure 3.** X-ray Diffraction measurements for 100-nm-thick W(solid) and  $WN_x$  (dotted) films, as labeled.

In another experiment, a series of  $B_4CN_x$  films of varying thickness were deposited in the S-Gun system described above using an  $N_2$  Gas Fraction of 6.4%. Films were deposited onto either Si (100) or 0.2-mm-thick glass (Corning #0211) substrates, and AFM measurements were made before and after film deposition. The resultant PSD curves are shown in Figure 4. We find that the rms surface roughness of the  $B_4CN_x$  films decreases with increasing film thickness (in contrast to the  $WN_x$  films just discussed), and furthermore the surface roughness is consistently less than the roughness of the underlying substrates in all cases; the PSD data shown in Fig. 4 indicate that these films thus act to reduce the very-high-spatial-frequency roughness of the underlying substrate, specifically for spatial frequencies greater than  $\sim 10 \mu m^{-1}$  (i.e., the spatial frequencies that matter most for optics designed for use at short X-ray wavelengths.<sup>2</sup>) For example, we find an rms surface roughness of approximately  $2.5\text{\AA}$  for these uncoated Si (100) wafers, while the rms surface roughness of a 100-nm-thick  $B_4CN_x$  film deposited onto such a substrate was found to be  $1.66\text{\AA}$ . As another – and perhaps more important – example, we find an rms roughness of order  $2.9\text{\AA}$  for the thin glass substrates studied here (which could be used to fabricate figured X-ray telescopes, for example<sup>14</sup>), while the roughness after deposition of 100 nm of  $B_4CN_x$  is  $2.19\text{\AA}$ ; again, from Fig. 4b it is clear that most of this reduction occurs at the highest spatial frequencies.

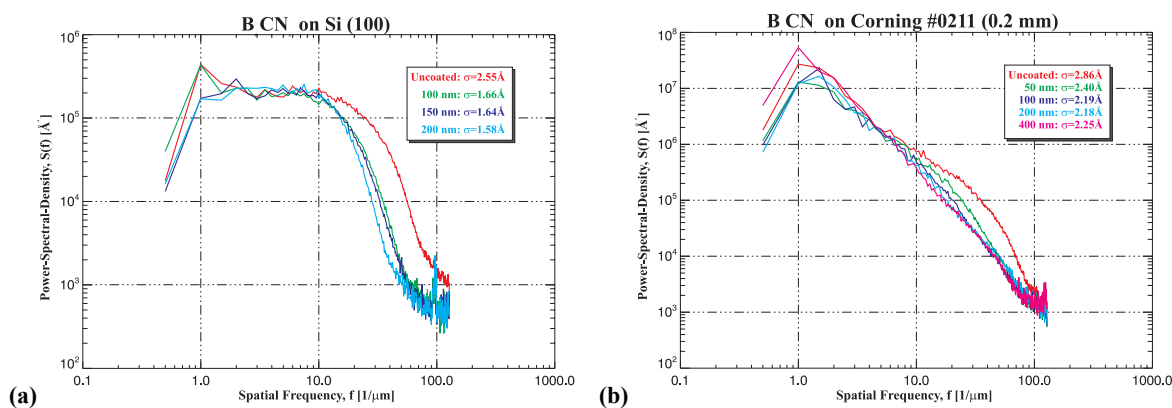


**Figure 4.** Power-Spectral-Density curves determined from atomic force microscopy, for  $B_4CN_x$  films as a function of thickness, as deposited onto (a) Si (100) wafers and (b) 0.2-mm-thick Corning #0211 glass sheet.

Based on the results shown in Fig. 4, we propose that these reactively-sputtered  $B_4CN_x$  films can thus be used as ‘smoothing layers’, which can be deposited onto X-ray mirror substrates (prior to the deposition of a single-layer or multilayer X-ray reflective coating) in order to reduce the high-spatial-frequency roughness that has the potential to scatter short-wavelength X-rays out of the specular direction. The resultant reduction in substrate roughness will thus give rise to a significant increase in X-ray reflectance and a decrease in scattered X-ray intensity, crucial parameters in the construction of astronomical X-ray telescopes, for example. The relatively low stress obtained for these films (e.g., Fig. 1) reduces the potential for coating adhesion failures that might otherwise occur.

### 3.2 W/B<sub>4</sub>C Multilayer Films

Driven by the encouraging results obtained for single-layer W and B<sub>4</sub>C films described above, we have also investigated the performance of both periodic and depth-graded W/B<sub>4</sub>C multilayer films deposited with and without nitrogen. Shown in Figure 5 are the XRR data obtained for short-period W/B<sub>4</sub>C multilayers containing N=40 bilayers, and having a period of  $d=11.25\text{\AA}$ . These films were both grown in the S-Gun system. For the film grown reactively, the N<sub>2</sub> Gas Fraction was once again set to 6.4%. The XRR results of Fig. 5 reveal that the reflected intensity at the 1<sup>st</sup> order Bragg peak near  $\theta=3.9^\circ$  is measurably higher for the film grown in the Ar/N<sub>2</sub> gas mixture relative to the film grown using only Ar gas, suggesting reduced interfacial roughness in the films grown reactively. Furthermore, the Kiessig fringes are also better defined in the case of the reactively-sputtered multilayer, also consistent with reduced interfacial and surface roughness. Fits to the XRR data suggest a small, but nevertheless significant reduction in interfacial roughness, from  $4.7\text{\AA}$  to  $4.4\text{\AA}$ .

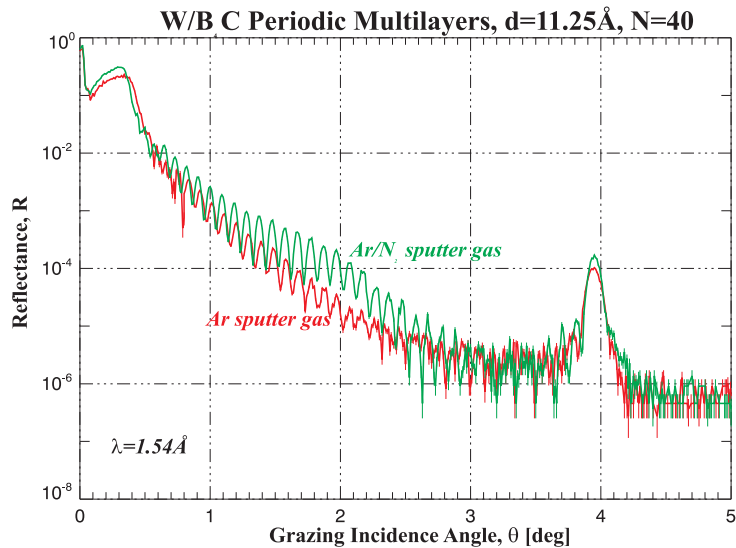


**Figure 5.** X-ray reflectance measurements for periodic W/B<sub>4</sub>C multilayers having 40 periods, with  $d=11.25\text{\AA}$ , deposited non-reactively using Ar gas, and reactively using an Ar/N<sub>2</sub> gas mixture, as labeled.

Shown in Figure 6 are the XRR data for depth-graded W/B<sub>4</sub>C films deposited in the Vactec deposition system with and without nitrogen. These particular multilayers contain N=200 bilayers, with bilayer thicknesses in the range  $d = 25 - 450\text{\AA}$ ; this coating is designed for operation up to  $\sim 12\text{ keV}$  at graze angles near  $\theta \sim 0.3 - 0.4^\circ$ , and thus would be suitable for use in an X-ray telescope such as the instrument currently proposed for NASA’s future Constellation-X astronomy mission.<sup>15</sup> The N<sub>2</sub> Gas Fraction was set to 9% for the reactively-sputtered multilayer. The XRR data shown in Fig. 6 are plotted on a linear scale, which better emphasizes the performance just above the critical angle in the range  $\theta = 0.5 - 1.0^\circ$ , which is the angular range that is best correlated with the performance at the design X-ray energies. It is clear from Fig. 6 that the reactively-sputtered multilayer has performance that is much closer to the design curve (also shown), with well-defined interference fringes, while the film deposited without nitrogen has much lower reflectance overall and poorly-defined peaks. (Note that there are no ‘conventional’ Bragg peaks in these depth-graded multilayers designed for broad-energy response.) The XRR results are again consistent with reduced interfacial roughness in the reactively-sputtered film.

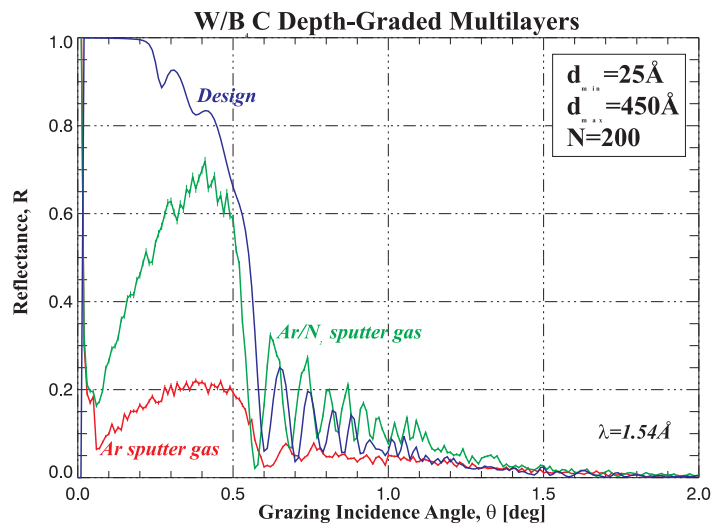


**Figure 6.** X-ray reflectance measurements for depth-graded W/B<sub>4</sub>C multilayers containing 200 bilayers, with  $d_{\min}=25\text{\AA}$  and  $d_{\max}=450\text{\AA}$ , deposited non-reactively using Ar gas, and reactively using an Ar/N<sub>2</sub> gas mixture, as labeled. The calculated response based on this multilayer design is also shown.

Wafer curvature measurements made on the same type of W/B<sub>4</sub>C depth-graded multilayers show a marked reduction in total film stress, from  $-1511\text{ MPa}$  for the non-reactively-sputtered *as-deposited* film, to a value of  $-421\text{ MPa}$  for the reactively-sputtered film. The large stress measured in the non-reactively-sputtered film is certainly sufficient to cause adhesion failures, and indeed the sample studied here, deposited onto a 3" Si wafer, already began to craze at the edges after just a few hours upon removal from the coating chamber; no crazing has been observed to date in the reactively-sputtered coating.

Finally, shown in Figure 7 are stress-vs-temperature data obtained on these W/B<sub>4</sub>C depth-graded multilayers deposited reactively and non-reactively. Both films show irreversible stress changes at  $\sim 90\text{ C}$ , with steady relaxation upon heating to  $300\text{ C}$ . These changes in stress may be due to one or more possible mechanisms, including chemical reactions at the interfaces, viscous flow and/or densification within the individual layers, etc.<sup>16</sup> In any case, the total change in stress ( $\Delta\sigma$ ) after heating to  $300\text{ C}$  is significantly less in the case of the reactively sputtered film:  $\Delta\sigma=177\text{ MPa}$  for the reactively-sputtered film versus  $\Delta\sigma=822\text{ MPa}$  for the non-reactively-sputtered film. (The linear cooling curves in both cases, as well as the linear portions of the heating curves from  $25$  to  $\sim 90\text{ C}$ , correspond simply to thermal stresses resulting from the difference in thermal expansion coefficient between the film and the substrate.)

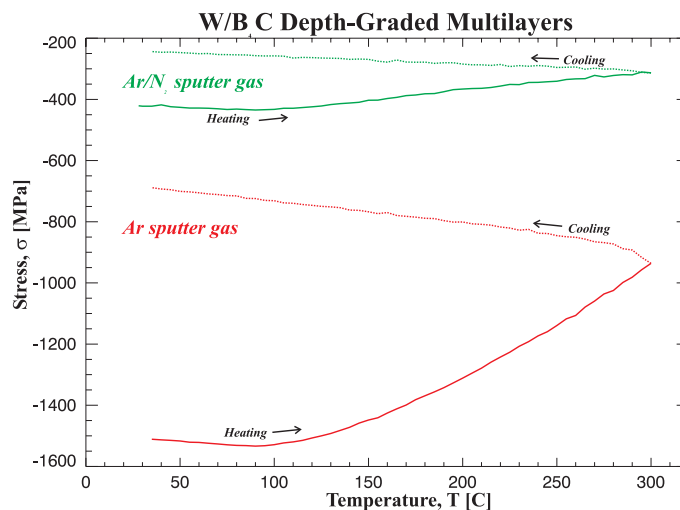


**Figure 7.** Stress-vs-temperature measurements for depth-graded W/B<sub>4</sub>C multilayers containing 200 bilayers, with  $d_{\min}=25\text{\AA}$  and  $d_{\max}=450\text{\AA}$ , deposited non-reactively using Ar gas, and reactively using an Ar/N<sub>2</sub> gas mixture, as labeled.

## 4. DISCUSSION

Reactive sputtering using nitrogen has been widely used for many years, principally for the production of stoichiometric (or near-stoichiometric) nitrides for electronic, mechanical and optical applications.<sup>17</sup> Nanometer scaled superlattices and multilayers composed of transition metal nitrides have been widely studied as well, as such coatings can achieve significant increases in hardness, thereby finding a variety of useful mechanical applications.<sup>18</sup> Reactive sputtering in nitrogen has also been recently used for the production of epitaxial CrN/ScN X-ray superlattices,<sup>19</sup> however in that case the specific aim was to increase the thermal stability and wear resistance of these coatings relative to conventional Cr/Sc X-ray multilayers, in order to facilitate their use in harsh environments.

In contrast to the past utilization of reactive sputtering with nitrogen just outlined, the research described here was designed specifically to reduce stress and roughness simultaneously in W, B<sub>4</sub>C, and W/B<sub>4</sub>C films – with little regard to chemical composition – in order to improve the X-ray performance of these coatings and to reduce the likelihood of stress-driven coating adhesion failures. Based on the experimental results presented above, we have demonstrated how these benefits have been realized in practice. We have also demonstrated reduced surface roughness (relative to the underlying substrate) in B<sub>4</sub>CN<sub>x</sub> films, also grown by reactive sputtering in nitrogen using a stoichiometric B<sub>4</sub>C sputter target; these B<sub>4</sub>CN<sub>x</sub> films therefore can be used as ‘smoothing layers’ in order to reduce the surface roughness of X-ray mirror substrates for spatial frequencies higher than  $\sim 0.10 \mu\text{m}^{-1}$ , i.e., the range of spatial frequencies that will scatter hard X-rays into non-specular directions in many practical applications.

In summary, we have found that deposition of WN<sub>x</sub> and B<sub>4</sub>CN<sub>x</sub> by reactive sputtering with nitrogen has a profound effect on the surface roughness and stress in these materials, presumably resulting from the corresponding changes in chemical composition and microstructure. These changes are manifest in multilayers containing WN<sub>x</sub> and B<sub>4</sub>CN<sub>x</sub> layers as well. In particular, the simultaneous reduction of film stress and roughness in both periodic and depth-graded W/B<sub>4</sub>C X-ray multilayers deposited reactively results in improved X-ray performance as well as improved coating adhesion.

Future research based on the results presented here may focus on the use of reactive sputtering with nitrogen for the fabrication of improved X-ray multilayer coatings comprising materials other than W and B<sub>4</sub>C. Specifically, multilayers containing C, Si, SiC, Co, Ni, Mo, or Pt layers are of particular interest for use at hard X-ray wavelengths, and the use of reactive sputtering may very well result in reductions in roughness and stress similar to those found for the W/B<sub>4</sub>C multilayers studied here.

## 5. ACKNOWLEDGEMENTS

This research was supported by NASA grants NNG06WC15G and NNG06HA04G.

## REFERENCES

- <sup>1</sup> D. G. Stearns, *J. Appl. Phys.* 65, 491 (1989)
- <sup>2</sup> D. L. Windt, W. K. Waskiewicz and J. E. Griffith, *App. Opt.*, 33, 2025-2031 (1994)
- <sup>3</sup> D. L. Windt, *J. Vac. Sci. Tech., A*, 18, 980 – 991 (2000)
- <sup>4</sup> J. A. Thornton, *J. Vac. Sci. Technol.* 11, 666-670 (1974)
- <sup>5</sup> R. Messier, A. P. Giri and R. A. Roy, *J. Vac. Sci. Technol. A* 2, 500 – 503 (1984)
- <sup>6</sup> D. L. Windt, E. M. Gullikson, C. C. Walton, *Opt. Lett.*, 27, 2212-2214 (2002)
- <sup>7</sup> Unpublished
- <sup>8</sup> D. L. Windt and W. K. Waskiewicz, *J. Vac. Sci. Technol. B*, 12, 3826-3832 (1994)
- <sup>9</sup> J. Dalla Torre, G. H. Gilmer, D. L. Windt, R. Kalyanaraman, F. H. Bauman, P. L. O’Sullivan, J. Sapjeta, T. Diaz de la Rubia, and M. Djafari Rouhani, *J. App. Phys.*, 94, 263 – 271 (2003)
- <sup>10</sup> H. Windischmann, *J. Vac. Sci. Tech. A*, 9, 2431-2436 (1991)
- <sup>11</sup> D. L. Windt, *Computers in Physics*, 12, 360 – 370 (1998)
- <sup>12</sup> The TOPO surface analysis software package is available at <http://www.rxollc.com/idl>
- <sup>13</sup> G. G. Stoney, *Proc. Roy. Soc. London*, A82, 172-175 (1909)
- <sup>14</sup> J. E. Koglin, C. M. Hubert, J. Chonko, F. E. Christensen, W. W. Craig, T. R. Decker, C. J. Hailey, F. A. Harrison, C. P. Jensen, K. K. Madsen, M. Pivovoroff, M. Stern, D. L. Windt, and E. Ziegler, *Proc. SPIE*, 5488 (2004)

<sup>15</sup> <http://constellation.gsfc.nasa.gov/>

<sup>16</sup> A. Witvrouw and F. Spaepen, in Kinetics of Phase Transformations, edited by M. O. Thompson, M. J. Aziz, and G. B. Stephenson (Materials Research Society, Pittsburgh, PA, 1991).

<sup>17</sup> 'Thin Film Processes II', edited by J. L. Vossen and W. Kern, Academic Press, Inc. San Diego, CA, 1991

<sup>18</sup> S.A. Barnett, Physics in Thin Films, Academic Press, New York, 1992; L. Hultman, Hard Nanostructured Coatings, Plenum Press, New York, 2005

<sup>19</sup> J. Birch, T. Joelsson, F. Eriksson, N. Ghafoor, and L. Hultman, Thin Solid Films, 514, 10 – 19 (2006)